Towards the development of synthetic vaccines against tuberculosis

Marino, L.

4

Synthesis and immunological evaluation of conjugates containing a TLR2 agonist

Laura Marino [1], Susan J.F. van den Eeden [2], Krista E. van Meijgaarden [2], Nico J. Meeuwenoord [1], Dmitri V. Filippov[1], Annemieke Geluk [2], Ferry A. Ossendorp [3], Gijs A. van der Marel [1], Jeroen D.C. Codée [1], Tom H.M. Ottenhoff [2]

[1] Department of Bio-organic Synthesis, Leiden University, Leiden, The Netherlands

[2] Department of Infectious Diseases, Leiden University Medical Center, Leiden, The Netherlands

[3] Department of Immunology, Leiden University Medical Center, Leiden, The Netherlands

4

Abstract

Despite the availability of the Bacillus Calmette-Guérin vaccine for the prevention of tuberculosis (TB), *Mycobacterium tuberculosis (Mtb)* remains one of the deadliest pathogens in the world. Novel vaccination strategies are required, and synthetic chemistry provides excellent tools to develop highly pure, homogenous and economical vaccines. Antigenic peptide epitopes are the smallest fragments in protein antigens recognized by immune cells. However, they are often poorly immunogenic by themselves. To overcome their poor immunogenicity, peptides can be formulated with adjuvants, or covalently linked to immunostimulatory molecules. Here, a panel of three synthetic peptide-conjugates was generated, with each containing a TLR2 ligand covalently attached to one of three antigenic peptides (p57 from the *Mtb* Rv1733c protein, p31 and p75 from the *Mtb* Rv2034 protein). These synthetic conjugates induced strong innate immune responses *in vitro* using human antigen-presenting cells. Most importantly, it is reported that one conjugate was more immunogenic *in vivo* when compared to the unconjugated admixture of peptide and TLR2 ligand. After subcutaneous vaccination in mice, the synthetic conjugate induced Th17 cellular responses and co-expression of multiple antigen-specific IgG subclasses. Furthermore, the conjugate was effective in reducing the bacterial load in the spleen of humanized, HLA-DR3 transgenic mice that had been intranasally infected with *Mtb* bacilli. These results suggest a promising role for molecularly defined TLR2 ligand-peptide conjugates as novel TB vaccine modalities, and provide additional support to the role of synthetic chemistry in aiding the development of highly pure and versatile vaccines.

Introduction

Tuberculosis (TB) is one of the top ten causes of death worldwide and is caused by aerosol infection with *Mycobacterium tuberculosis (Mtb)*.[1] Novel improved vaccination strategies replacing or complementing current Bacillus Calmette-Guérin (BCG) vaccinations, are required to reduce the TB burden.[2] According to the latest epidemiological studies reported by the World Health Organization, the most affected populations are those in developing countries, with the majority of infection cases in India (26%), Indonesia (8.5%), China (8.4%), the Philippines (6.0%), Pakistan (5.7%) and Nigeria (4.4%).[1] The development of an efficacious and inexpensive vaccine against *Mtb* would accelerate the global efforts to halt the spread of this disease to vulnerable populations.

Fully synthetic compounds, with their economical, versatile and robust manufacturing processes, represent a promising resource which can find application in the field of vaccine development, as illustrated by the fast de novo design and production of SARS-COV2 synthetic vaccines.[3,4] The rational design of such modern synthetic vaccines relies on the identification of suitable antigens to induce selective immunity towards a specific pathogen.[5] Proteins and peptides are the most common antigenic units that are recognized by antigen-presenting cells (APCs) and that are subsequently presented to B and T cells, key players for the development of humoral and cellular immunity.[6]

Usually, such antigens by themselves are poorly immunogenic when injected, and generally only induce weak immune responses if employed as a single entity. The combination of antigenic proteins or peptides with immune-stimulatory molecules, called adjuvants, is a proven successful strategy to circumvent the issue of poor immunogenicity.[7,8] Synthetic long peptides (SLPs) have been successfully employed to design therapeutic vaccines against the *Human Papillomavirus*.[9]

Recently, synthetic conjugates containing antigen(s) covalently attached to the adjuvant(s) of choice in the form of a single molecular construct, have been studied and shown to induce efficient antitumor immunity.[10,11] This Chapter reports on the application of a similar simple approach for the discovery of synthetic vaccines against TB. The novel molecular constructs employed in these studies were designed to include a toll-like receptor 2 (TLR2) ligand which would act as adjuvant, and one of three different synthetic long peptides (SLPs) as *Mtb* antigens. These conjugates were evaluated to determine the robustness of the conjugation strategy and the effect of conjugation on the biological outcome (see Figure 1 for a schematic overview of the study design).

TLR2 is a pattern recognition receptor (PRR) mainly expressed on the cell surface of antigen-presenting cells, such as dendritic cells and macrophages, and it is known to interact with bacterial lipoproteins. Upon agonist engagement with TLR2, a

TIRAP/MyD88 activation pathway is initiated which results in transcription of several inflammatory genes.[12] This receptor is often expressed as a heterodimer in combination with TLR1 or TLR6.[13]

Synthetic vaccines comprising TLR2 ligands have been shown to induce strong immune responses. In 2014, Pam_3CysSK_4, a TLR2/TLR1 ligand, was covalently attached to melanoma or lymphoma tumor derived epitopes and shown to promote $CD4^+$ and $CD8^+$ T cell responses, which correlated with *in vivo* anti-tumor activity.[14] In 2016, the same research group employed UPam (also known as Amplivant), also a TLR2/TLR1 ligand, in the form of a synthetic conjugate to stimulate human monocyte-derived dendritic cells and specifically activate cancer patient-derived T cells.[15] Most importantly, pulmonary immunization of C57BL/6 mice using the TLR2/TLR6 ligand Lipokel (a derivative of Pam_2Cys linked to the Ni^{2+}-chelating entity 3NTA) conjugated to *Mtb*-derived proteins was shown to provide protection after low dose *Mtb* challenge (100 CFU), while inducing IFN-γ^+ T lymphocytes and IgG antibodies.[16]

Given its enhanced immune-stimulatory ability as compared to the more popular Pam_3CysSK_4 adjuvant, UPam was chosen for the construction of the conjugates described in the present chapter.[17] This compound can be easily conjugated to SLPs using a synthetic strategy that involves exclusively the use of solid phase synthesis, which is a common methodology employed for the generation of SLPs. Compared to the more classical wet chemistry methods, solid phase synthesis offers several advantages, including simplicity and speed (since all reactions are carried out in a single reaction vessel), efficiency and cost-effectiveness (since it can easily be automated and the large losses normally encountered during isolation and purification of intermediates are reduced).[18]

The chosen Mtb-derived SLPs used for conjugation to UPam are HLA-DR3 binding peptide sequences, with HLA-DR3 being a major class II allele that is present in about 20% of the human population.[19] The selected peptides were shown to be presented to HLA-DR3 restricted T cells in humans or in transgenic mice.[20–23] They belong to either the Rv1733c or Rv2034 proteins, expressed during latent and inflammatory pulmonary infection, respectively. These two proteins were both shown to be strongly recognized by T cells from mycobacteria-exposed individuals.[24,25] The *in vivo* vaccine potential of Rv1733c- and Rv2034-derived synthetic long peptides, administered subcutaneously to HLA-DR3/Ab^0 mice in admixture with a toll-like receptor 9 (TLR9) agonist, has been previously shown.[21,22]

In the present study, three conjugates containing UPam covalently linked to the p57 peptide (Rv1733c a.a. 57-84), p31 peptide (Rv2034 a.a. 31-60) and the p75 peptide (Rv2034 a.a. 75-105) were synthesized. It was demonstrated that these synthetic compounds induced strong immune responses *in vitro* using human antigen-presenting cells. Most importantly, the vaccine potential of the p57-UPam conjugate

was revealed in a preliminary study following challenge of HLA-DR3 transgenic mice with live *Mtb*, which resulted in a significant reduction of the bacterial load in the spleen of vaccinated mice. This finding correlated with the induction of a Th17 cellular response and strong antibody titers *in vivo*.

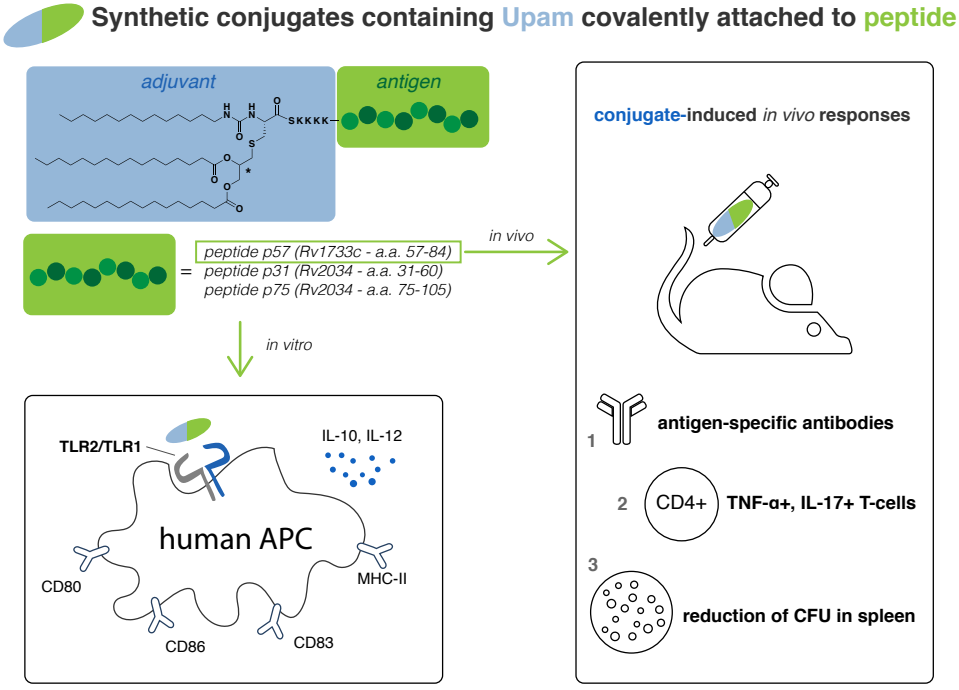

Figure 1 – Visual representation of synthetic conjugates generated and key immunological assays performed. Three conjugates were synthesized using in-line solid phase peptide synthesis, containing a TLR2 ligand (UPam) and one of three peptides contained in either Rv1733c or Rv2034 *Mtb*-derived protein. The three conjugates were assayed for their ability to activate human antigen-presenting cells (monocyte-derived dendritic cells and macrophages type 1 and 2) *in vitro*. One selected conjugate was further studied for its ability to induce humoral and cellular responses *in vivo*, and was shown to significantly reduce the bacterial load in the spleen of immunized mice that were live *Mtb* challenged.

Results

Synthesis of peptides and conjugates

The peptides were synthesized using standard Fmoc automated solid-phase synthesis. The use of pseudoproline derivatives for the generation of the p57 and p75 peptides was chosen to minimize aggregation during the stepwise assembly of these two hydrophobic peptides. The resulting yields after HPLC purification (12.1 and

14.1% for the p57 and p75 peptides, respectively) were comparable to that calculated for the water-soluble p31 peptide (12.0%). Synthesis of the peptide-UPam conjugates was performed according to an inline solid-phase synthetic protocol. In summary, the peptide was generated by Fmoc automated solid-phase synthesis and, without cleavage from the resin, it was immediately elongated with a known cysteine derivative (see materials and methods section) in the presence of oxyma pure and DIC. Subsequent washing and Fmoc-removal steps were followed by treatment with tetradecyl isocyanate to complete synthesis of UPam moiety. The conjugate was then cleaved from the resin and simultaneously deprotected. The p57, p31 and p75 UPam conjugates were obtained with overall yields of 3.3, 7.3 and 2.8%, respectively, after HPLC purification.

Dynamic light scattering measurements

The peptides have different physicochemical properties, including a different net charge at pH 7 and different water solubility. As determined using dynamic light scattering (DLS), the p57 peptide forms nanoparticles with hydrodynamic diameter of 170 nm and very low polydispersity index (PDI), peptide p31 forms nanoparticles with hydrodynamic diameter of 238 nm and intermediate PDI, peptide p75 forms bigger nanoparticles with hydrodynamic diameter of 986 nm and very high PDI.

Table 1 – Dynamic light scattering measurements for peptides in deionized water (20 μM):

	net charge at pH 7*	**particle size (nm)**	**PDI**	**derived count rate (kcps)**
pept. p57	2.3	170	0.062	4658
pept. p31	3.1	238	0.200	52**
pept. p75	-1	986	0.402	705

*calculated using Pepcalc.com prediction software

**The good water solubility of peptide p31, as predicted using Pepcalc.com, may be responsible for the low derived count rate calculated using the zetasizer software v7.13 (Malvern Panalytical).

In vitro evaluation using TLR2 ligand-peptide conjugates

The commercially available HEK-293-hTLR2 and HEK-null cell lines were used to probe binding of p57-UPam, p31-UPam and p75-UPam conjugates. The HEK-293-hTLR2 cell line is a reporter cell line transfected to over-express human TLR2

protein, while the HEK-null cell line is the not-transfected negative control cell line.[1] HEK-293-hTLR2 cells were stimulated with ligands able to engage the TLR2 receptor and responses determined by measuring the release of IL-8 in the cell supernatant by ELISA. The free UPam adjuvant was used as a positive control, and a reference dose-response curve using this compound was generated. After 20 hours of stimulation of HEK-293-hTLR2 cells all three synthetic conjugated peptides induced production of IL-8 in a concentration dependent manner, as shown in Figure 2. The p31-UPam conjugate induced response that closely paralleled the physiological response to free UPam adjuvant. The responses induced by the p57-UPam and p75-UPam conjugates were lower than that of UPam, but significantly higher than the background. The absence of any detectable amount of IL-8 in the cell supernatant of HEK-null cells stimulated with UPam or conjugates (data not shown) confirmed that the responses were strictly TLR2 dependent.

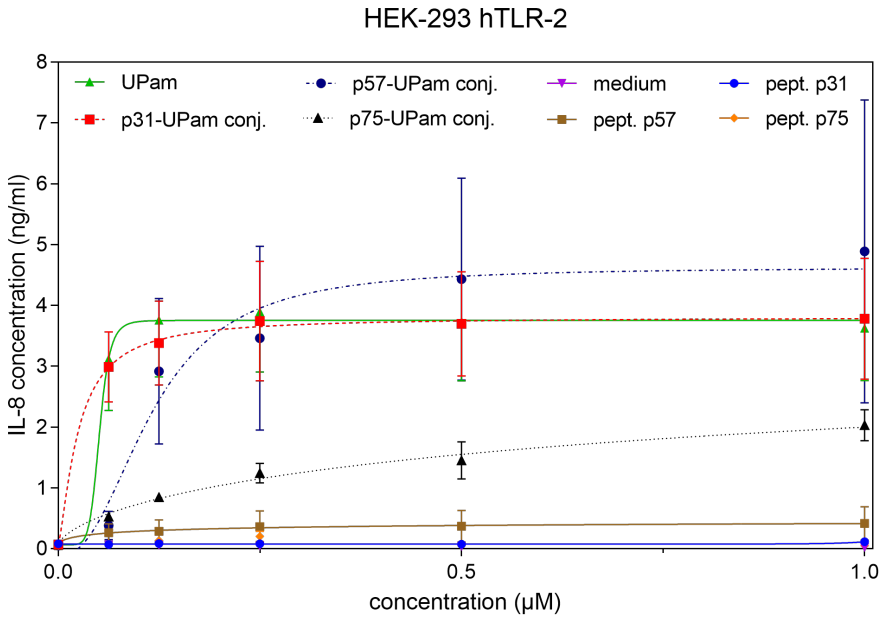

Figure 2 – Amount of IL-8 released by HEK-293 hTLR2 cells as a measure of TLR2 activation. HEK-293 cells expressing human TLR2 were stimulated with soluble UPam adjuvant, free peptides or UPam-conjugated peptides for 20h. HEK-293 null cells, not transfected with human TLR2, were used as negative control cell line and stimulated according to the same protocol as HEK-293 hTLR2 cells. NF-κB activation was determined by measuring secreted IL-8 in the cell supernatants by ELISA. Dots represent mean + SEM of duplicates from two independent experiments. Curves were interpolated using a non-linear regression model with 4 parameters as calculated using GraphPad Prism software.

[1] Both cell lines express TLR1, a receptor which can form heterodimers with TLR2.

To further evaluate the TLR2 ligand-peptide conjugates, monocytes were isolated from healthy human donors, differentiated into dendritic cells (GM-CSF/IL-4), macrophages type 1 (GM-CSF) or macrophages type 2 (M-CSF). As quality control, their archetypical cell surface marker phenotypes were characterized by CD1a, CD14, CD11b and CD163 expression.[26,27] These antigen-presenting cells were then stimulated for 24 hours using synthetic conjugates, free peptides or free UPam adjuvant. Lipopolysaccharide (LPS) was used as positive control. Cells were assayed for the expression of activation markers, T cell co-stimulatory molecules and MHC-II molecules using flowcytometry. Furthermore, cell supernatants were analyzed via ELISA to determine the level of IL-12p40 and IL-10 cytokines.

The three conjugates, the UPam adjuvant and the LPS control were able to activate both dendritic cells and macrophages. The median fluorescence intensity (MFI), as obtained from flow cytometry measurements, displayed in Figure 3 for one selected cell surface marker per cell type, exemplifies the extent of cellular activation (histograms for CD80, CD83, CD86 and MHC-II are shown in the supporting Figures S1, S2 and S3). Free UPam and all conjugates induced upregulation of CD86 on the cell surface of monocyte-derived dendritic cells (moDCs) and upregulation of CD80 on macrophages in a dose dependent manner, while corresponding free peptides neither promoted activation nor enhanced the expression of these markers.

Cell activation induced by UPam and synthetic conjugates was confirmed by analysis of cytokine levels in the supernatant of tested antigen-presenting cells (see Figure 4). In this analysis, it was observed that the p57-UPam and p75-UPam conjugate stimulated dendritic cells to release higher amounts of IL-12p40 (with mean values of 47 and 27 ng/ml respectively) and IL-10 (with mean values of approximately 1.1 ng/ml for both) at their highest experimental concentration (20 μM), when compared to the p31-UPam conjugate (mean values of 1.5 ng/ml IL-12p40 and 0.1 ng/ml IL-10). Cell viability was measured by flow cytometry, and no difference was observed between the p31-UPam conjugate and UPam. Nevertheless, a higher amount of cytokines was detected in the case of cell stimulation using the intermediate concentration of the p31-UPam conjugate as compared to the 20 μM concentration. As expected, the unconjugated peptides did not induce cytokine production.

Stimulation of macrophages type 1 with the UPam adjuvant or the conjugates resulted in production of only IL-12p40, as expected, with mean values ranging from 0.3 to 2.1 ng/ml, while stimulation of macrophages type 2 as expected resulted in production of only IL-10, with mean values ranging from 0.5 to 3.0 ng/ml. Stimulation with unconjugated peptides did not induce any detectable amount of tested cytokines.

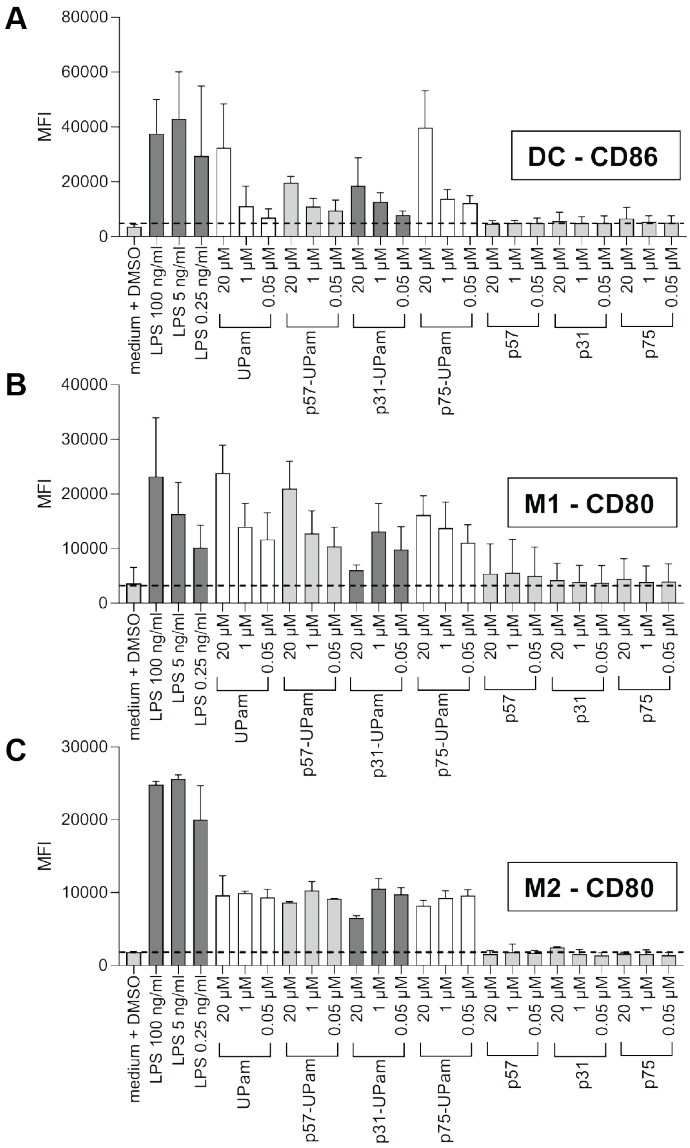

Figure 3 – Expression of selected activation markers by APCs stimulated with UPam conjugates and controls. Human monocyte-derived DCs, M1 and M2 cells were stimulated with soluble UPam adjuvant, free peptides or UPam-conjugated peptides for 24h. Expression levels of activation and T cell co-stimulatory markers were measured by flow cytometry. Bar plots represent the mean value + SD (n = 3 donors) of the median fluorescence intensity (MFI) of selected surface markers, as calculated using GraphPad Prism. LPS was used as a positive control. **(A)** MFI of the CD86 activation marker on human dendritic cells; **(B)** MFI of the CD80 co-stimulatory marker on human macrophages type 1; **(C)** MFI of the CD80 co-stimulatory marker on human macrophages type 2.

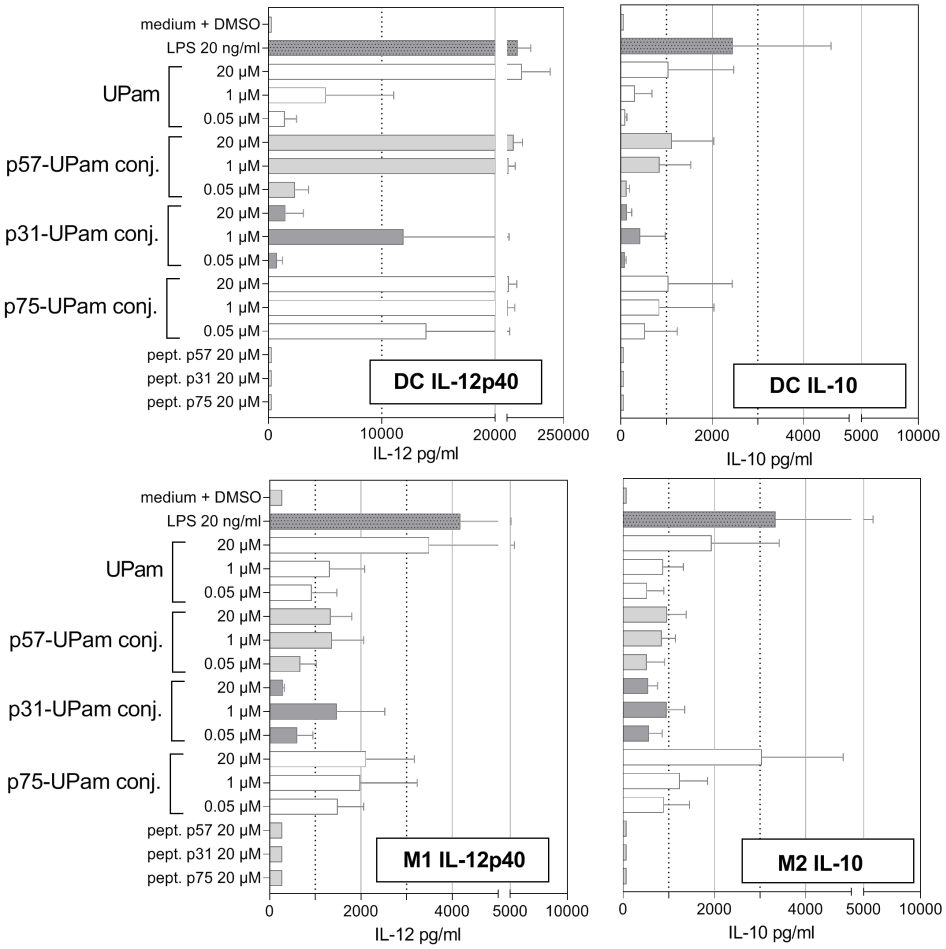

Figure 4 - Cytokine production profile of human monocyte-derived APCs stimulated for 24 hours with single adjuvant, free peptides or UPam-conjugated peptides thereof as measured by ELISA. LPS (20 ng/ml) was used as a positive control. Bar graph indicate the amount of IL-10 and IL-12p40 detected in the supernatant of macrophages and dendritic cells. No IL-10 was detected in the cell supernatant of macrophages type 1, and no IL-12p40 was detected in the cell supernatant of macrophages type 2 (data not shown). Error bars represent mean + SD of duplicates from three donors as calculated using GraphPad Prism.

To study unwarranted possible inhibitory effects of conjugation on antigen-presentation by human antigen presenting cells, on PBMC's or GM-CSF/IL-4 differentiated monocyte-derived dendritic cells, T cell assays were performed, measuring activation through proliferation by [^{3}H]-thymidine incorporation.

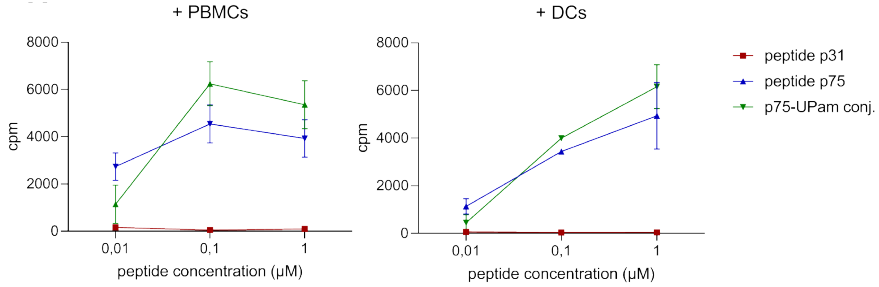

Figure 5 - Antigen-presentation to T cells. The experiment was performed by co-culturing T cells with HLA class II matched moDCs or PBMCs in the presence of the Rv2034 peptide p75 or p75-UPam conjugate. The T cell clone used in this study is specific for the Rv2034 p75 peptide, Rv2034 p31 peptide was used as a negative control. T cell proliferation was measured after 96 hour peptide stimulation using [^{3}H]thymidine incorporation and is expressed as counts per minute (cpm). Values represent mean + SD of triplicate measurements from a representative experiment, as calculated using GraphPad Prism.

The HLA-DR3 restricted CD4$^+$ T cell clone specific for the *Mtb* antigen Rv2034 (peptide 81-100), was cocultured with antigen-presenting cells in the presence of free p75 peptide or UPam-conjugated p75 peptide. Additionally, the p31 peptide originating from the same Rv2034 protein and its UPam conjugate were included in the assay as negative controls (Figure 5).

The p75-UPam conjugate induced a dose-dependent T cell proliferation when presented to the CD4$^+$ T cell clone by HLA-DR matched APCs, as shown in Figure 5. Stimulation with p75-UPam conjugate showed comparable T cell proliferation levels as from p75 peptide stimulation for both PBMCs and DCs as antigen-presenting cells.

In vivo evaluation using TLR2 ligand-peptide

An HLA-DR3 transgenic mouse model, genetically lacking expression of murine MHC class II (I-A) molecules (HLA-DR3/Ab^0) has been previously used for *in vivo* induction of HLA-DR3 restricted Rv1733c derived p57 peptide specific T cell responses using subcutaneous (s.c.) SLP vaccination.[22,28] Here, this model was used to evaluate the *in vivo* immunogenicity of the p57-UPam conjugate compared to an equimolar mixture of unconjugated p57 peptide and UPam adjuvant. Intracellular IFN-γ, TNF-α and IL-17 production by CD4$^+$ CD44$^+$ T cells was measured by flow-cytometry after *in vitro* stimulation of splenocytes with either the p57 peptide antigen or with the original recombinant *Mtb* Rv1733c protein. The expression of CD44 was used as a marker of T cell activation. After antigen encounter, T cells rapidly up-regulate CD44 and its expression is also maintained in memory T cells.[29]

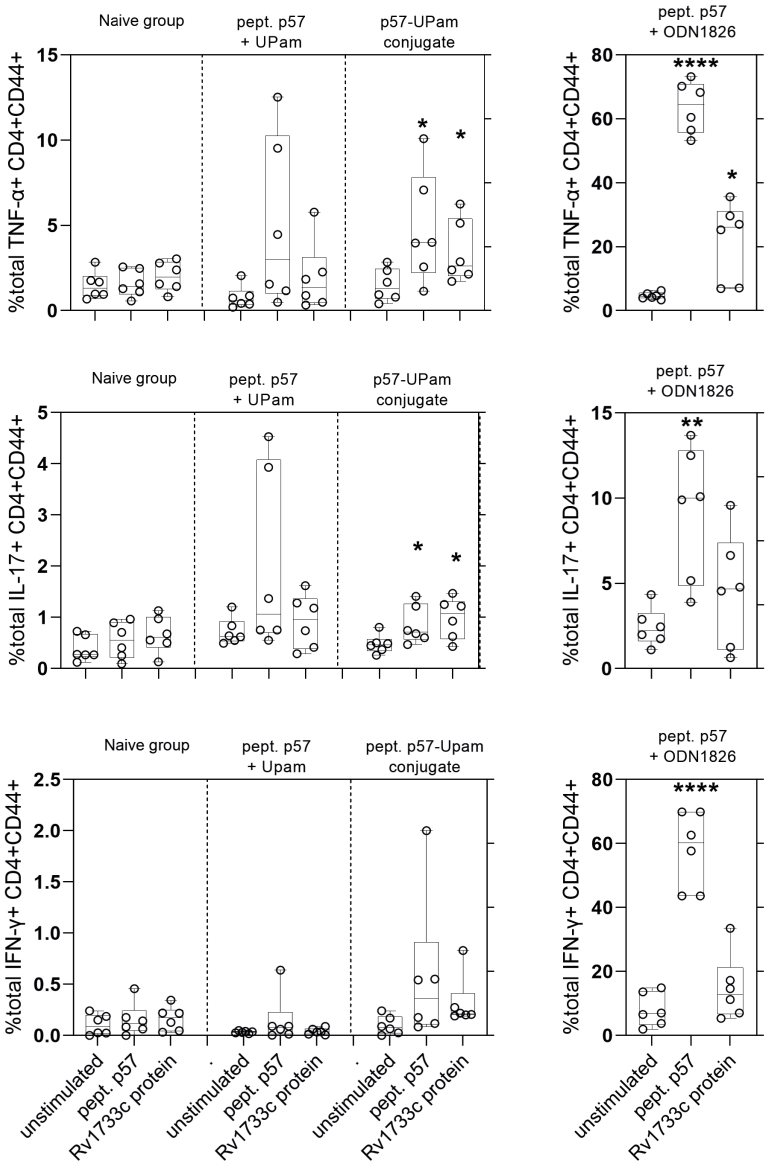

Figure 6 – Intracellular cytokine production by splenic T cells. Intracellular IL-17, TNF-α and IFN-γ production by $CD4^{+}CD44^{+}$ T cells was measured via flow-cytometry after in vitro stimulation of splenocytes with either peptide p57 (5 µg/ml) or Rv1733c recombinant protein (5 µg/ml). Mice (n=6) were injected three times with either PBS as negative control, peptide p57 (40 nmol) in admixture with ODN1826 (8 nmol) as positive control, peptide p57 (40 nmol) in admixture with UPam adjuvant (40 nmol) or peptide p57-UPam conjugate (40 nmol). Splenocytes were obtained two weeks after the last immunization. Statistical significance was calculated using a paired t-test as calculated with GraphPad Prism software (****$p < 0.0001$, **$p < 0.01$, *$p < 0.05$).

T cells from mice immunized with the p57-UPam conjugate were responsive to both the reference peptide p57 and to the Rv1733c recombinant protein *ex vivo*, as indicated by the significant increase in percentage of IL-17$^+$CD4$^+$CD44$^+$ and TNF-α^+CD4$^+$CD44$^+$ T cells (see Figure 6). Although a similar trend could be observed for the group of mice immunized with a mixture of peptide p57 with UPam, the results were not statistically significant. The group immunized with a mixture of peptide p57 with ODN1826 was used as positive control for the experiment, as it has been previously shown this to induce strong Th1 responses. This was here confirmed by the detection of significant numbers of IFN-γ^+CD4$^+$CD44$^+$ T cells by intracellular cytokine staining analysis for spleen of mice immunized with positive control. However, neither of the two UPam treatments induced expansion of IFN-γ positive T cells upon *ex vivo* antigen re-encounter, as shown in Figure 6.

Antigen specific total Ig antibodies were detected in the sera of mice immunized with either p57/adjuvant mixture or p57-UPam conjugate. The results revealed significantly higher antibody titers following vaccination with the conjugate (see Figure 7) compared to the unconjugated mixture, suggesting superior immunogenicity of the conjugated p57.

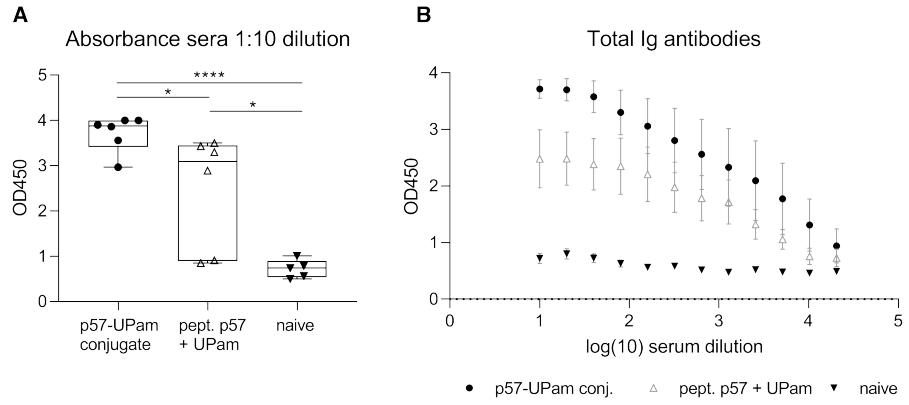

Figure 7 – Antibody production in the sera of immunized mice. Measurement of antigen-specific total Ig antibodies from sera of mice (n=6) immunized with peptide p57-UPam conjugate (40 nmol), peptide p57 (40 nmol) in admixture with UPam adjuvant (40 nmol) or treated with PBS only (naïve group). Plate-bound peptide p57 antigen was used for the Ig antibodies assay. **(A)** Box plots representing absorbance (OD450) corresponding to amount of antigen-specific total Ig antibodies and measured for sera diluted 10 times (n = 5 for naïve, n = 6 for the other groups). Statistical significance was calculated using unpaired t-test as calculated with GraphPad Prism software (****$p < 0.0001$, *$p < 0.05$). **(B)** Dose-response dot plots representing mean + SEM of absorbance measurements of the antigen-specific total Ig antibodies from 5 or 6 mice as calculated using GraphPad Prism.

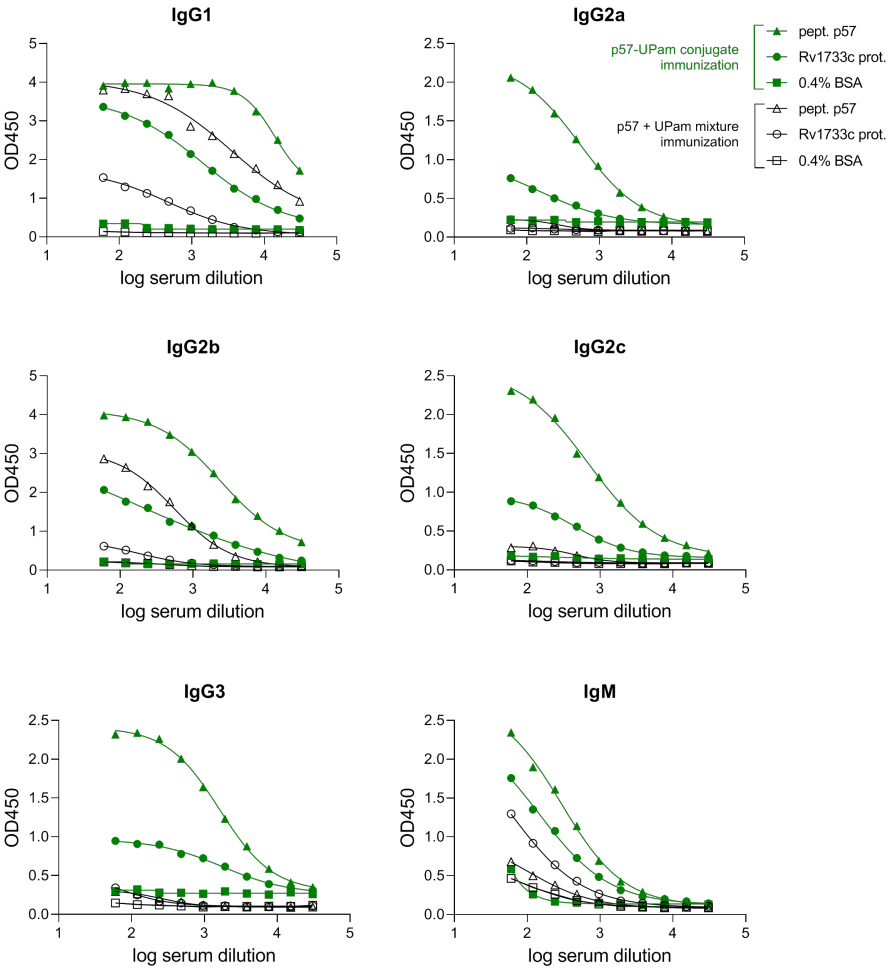

Figure 8 – Antibody subtypes in murine sera. Measurement of antigen-specific antibody isotypes from serum of mice (n=6) immunized with peptide p57-UPam conjugate or peptide p57 plus UPam mixture. Antigen-specific antibodies were measured using plate-bound peptide p57 or recombinant protein (Rv1733c). Mean data from sera of all mice (n=6 for peptide p57-UPam conjugate immunization; n=4 for peptide p57 plus UPam mixture) are shown. Curves were interpolated using a non-linear regression model with 4 parameters as calculated using GraphPad Prism. Data from the sera of each mouse are shown in the supplementary information.

Subsequent comparison of antibody titers between the two groups indicated a highly diversifying response between vaccination with the p57-UPam conjugate and unconjugated p57 with UPam. As shown in Figure 8, p57-UPam conjugate immunization induced antigen-specific IgG1, IgG2a, IgG2b, IgG2c, IgG3 and IgM recognizing not only the synthetic peptide, but also the Rv1733c recombinant

protein. This diversified antibody response was detected for all immunized mice. For comparative purposes, antibody subtypes in mice immunized using the mixture of peptide with adjuvant are also depicted in Figure 8. In this case, only four out of six mice vaccinated with the mixture of peptide with UPam developed antigen-specific Ig antibodies and the response was less diverse, with IgG1, IgG2b and IgM as main subtypes present in sera of mixture immunized mice. Thus, conjugation of p57 to UPam strikingly enhances its immunogenicity and also impacts the quality of the antibody subclass responses.

The vaccine potential of the p57-UPam conjugate was further evaluated in a prophylactic vaccination / *Mtb* challenge model using the same HLA-DR3 transgenic mouse model. Following a vaccination with BCG as positive control, or three times p57 with 2 weeks intervals, as described in the materials and methods section, mice were intranasally infected with 10^5 *Mtb* H37Rv. Six weeks later the spleen and lungs of infected mice were analyzed to determine the bacterial load by enumeration of the colony forming unit (CFU). Immunization with peptide p57 or UPam alone did not significantly reduce the CFU load in the spleen nor in the lungs (see Figure 9). As additional positive control next to BCG, vaccination with peptide p57 and ODN1826 was studied.

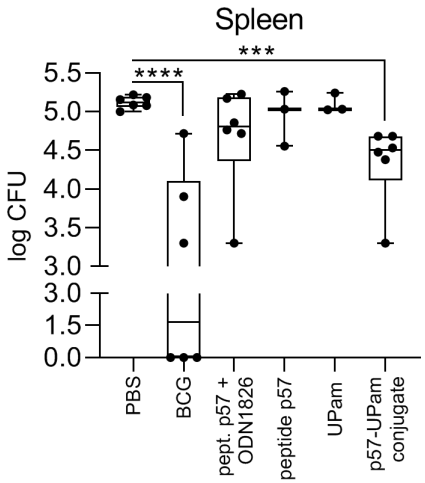

Figure 9 – Bacterial load in the spleen of immunized mice. Protective efficacy against *Mtb* in the spleen of mice that were immunized s.c. for 3 times with 2 weeks interval. Mice (n=6) were immunized with a mixture of peptide p57 (40 nmol) with ODN1826 (50 µg/ml) as adjuvant control, peptide p57-UPam conjugate (40 nmol) or mice (n=3) were treated with UPam adjuvant (40 nmol) or peptide p57 (40 nmol). Six weeks later, the mice were challenged intranasally with *Mtb* H37Rv (10^5 CFU). Alternatively, the mice received 10^6 CFU BCG s.c. 12 weeks before challenge. Colonies in lungs (data not shown) and spleen were counted after 3 weeks of incubation at 37°C. Statistical significance with reference to the naive group was determined by ANOVA with Tukey's multiple comparisons test (****$p < 0.0001$, ***$p < 0.001$). Box plots were generated using GraphPad Prism.

While BCG vaccination induced a significant reduction of the CFU in both the spleen and the lungs, immunization with peptide and ODN1826 did not, despite its impressive induction of T cell immunity (Figures 6A, 6B). In contrast, immunization with the p57-UPam conjugate resulted in a significant decrease in the number of CFU in the spleen of vaccinated mice, indicative of a systemic immune response to this construct that was conjugation dependent (since neither free p57 peptide nor free adjuvant were effective), and involving both T cells as well as strong antibody induction.

Discussion

Mycobacterium tuberculosis remains one of the deadliest pathogens worldwide. The only currently available vaccine, BCG, presents several limitations including its failure to induce robust and consistent protection.[30,31] Additionally, the burden of TB is especially afflicting populations in countries with fragile or developing economies The discovery of efficient synthetic vaccines against TB would hold promise of inexpensive and accessible vaccine for everyone. Despite their ease of manufacturing, versatility and improved safety profile as compared to inactivated or attenuated live vaccines, it was not until 2020 that two synthetic vaccines received their first historic emergency use authorization, with the liposomal mRNA vaccines against SARS-CoV-2 by BioNtech/Pfizer and Moderna.[3,4,32–34] One of the reasons for the delayed commercialization of fully synthetic vaccines is that their development has started later than that of attenuated/inactivated vaccines; another being the modest, yet growing, body of data available on the immune mechanisms of action involved in protection.[35–38] In general terms, rational design of fully synthetic vaccines requires the selection of relevant targets, the definition of a strategy to preserve/enhance immunogenicity of the synthetic molecule which acts on the selected target, and the verification of its mode of action. The present study provides evidence for the potential of rationally designed synthetic vaccines to induce protective immunity within the context of *Mtb* infection.

The conjugates here presented are designed to target human antigen-presenting cells in a TLR2-dependent manner. Previous studies have shown the beneficial effect of using TLR2 agonists to the induction of strong cellular immune responses, correlated to the reduction of tumor growth *in vivo* or protection against *Mtb*.[16,39] In this context, the immune-stimulatory potential of conjugates containing the TLR2/TLR1 ligand UPam covalently linked to one of the three following peptides was assessed: the p57 peptide (Rv1733c a.a. 57-84) for *in vivo* mouse studies, p31 peptide (Rv2034 a.a. 31-60) and the p75 peptide (Rv2034 a.a. 75-105) for *in vitro* human studies. This strategy allowed for co-delivery of antigen and adjuvant, which has been shown to improve immunogenicity as compared to delivering the two

separately, with the possibility to modify the chemical structure by linking additional moieties to increase immunogenicity or modulate solubility.[40] Additionally, synthetic conjugate vaccines can be generated with high purity and homogeneity. However, this strategy presents the risk of loss of immune-stimulatory potential of the adjuvant after conjugation to the peptide, or the impairment of antigen-presentation.

Despite the big differences in physicochemical properties of the three peptides selected in this study[2], it is shown that all generated conjugates retain the ability to interact with the TLR2 receptor. Using a HEK-293 cell line over-expressing human TLR2, the extent of binding of the novel conjugates to the receptor was assessed. Differences in potency and efficacy of binding were observed, possibly reflecting the different physicochemical properties of the three conjugates.

Typically, synthetic long peptides require processing through antigen-presenting cells for presentation to cognate T cell. To verify that conjugation did not affect APC processing, a human Rv2034-specific $CD4^+$ T cell clone that recognizes the epitope within the p75-UPam conjugate was employed for T cell proliferation and activation studies.

Comparable T cell proliferation levels were observed upon stimulation of monocytes, or alternatively dendritic cells, loaded with the p57-UPam conjugate or with the corresponding free SLP peptide. This observation was supported by flow cytometry analysis of the demonstrating increased expression levels of CD154 and IFN-γ by $CD4^+$ T cells. These studies indicated that the efficacy of antigen-presentation was not impaired by conjugation of the p75 peptide to UPam. A similar finding was reported by Zom *et al.* in 2016, where the HPV16-specific $CD4^+$ T cell clones were activated by peptide and UPam-conjugate to a comparable extent.[15]

The immune-stimulatory potential of the three conjugates was assessed *in vitro* by stimulating human monocyte-derived dendritic cells and macrophages (type 1 and type 2), and analyzing activation and T cell costimulatory markers together with production of the IL-12 and IL-10 cytokines.

Previous reports have indicated the presence of both IL-12 and IL-10 in the supernatant from moDCs stimulated with various TLR2 ligands.[15] While the role of IL-12 has been unequivocally defined as pivotal in the induction of pro-inflammatory responses and specific cellular immunity, that of IL-10 mostly confers anti-inflammatory and regulatory activity.[41–43]

As expected, stimulation of moDCs resulted in production of IL-12p40 and IL-10 cytokines. A relatively higher production of IL-12p40 was detected upon stimulation with two of the three conjugates (p57-UPam and p75-UPam) as compared to the other (p31-UPam conjugate), with the highest cytokine levels induced by the

[2] See their diverse predicted net charge, solubility and by the measurement of their hydrodynamic diameter (Table 1).

p57-UPam conjugate. A similar observation was indeed reported for conjugates containing the same adjuvant but different peptides.[15] This was not the case for the level of IL-10, which was produced in similar amounts across conjugate groups. It is additionally reported that IL-12 and IL-10 were released upon stimulation of macrophages type 1 and type 2, respectively, providing further evidence for the ability of these constructs to induce activation of these important cell types.

Interestingly, the p31-UPam conjugate induced an unconventional dose-response effect as compared to the UPam and to the other conjugates. It is highly unlikely that cell death caused the observed difference in response, as cell viability for moDCs treated with this conjugate was not different than with UPam alone. These results could be related, instead, to the different physicochemical properties of the peptides that are included in such constructs.

Additionally, this chapter reports evidence that free UPam and conjugates induced upregulation of CD86 on the cell surface of moDCs and upregulation of CD80 on macrophages in a dose dependent manner, while corresponding free peptides neither promoted activation nor enhanced the expression of these markers.

The *in vivo* immunogenicity of the p57-UPam conjugate was determined using an HLA-DR3/Ab^0 transgenic mouse model. Subcutaneous immunization with the conjugate was compared to immunization with an equimolar mixture of peptide and UPam. Additionally, a mixture of peptide with the TLR9 ligand ODN1826 was used as positive control, with previous work showing that this combination induced a Th1-polarized cellular response *in vivo*.[21,22]

Mice were immunized three times on a two weeks interval schedule, and, two weeks after the last immunization, draining lymph nodes and splenocytes were examined for CD4$^+$ T cell responses both *ex vivo* and after antigen restimulation. Evidence of the beneficial effect of CD4$^+$ T cell responses in containment of *Mtb* have been extensively provided in the last years, with a strong focus on Th1/Th17 polarized cellular responses.[44,45] More recently a renewed interest in the interplay between cellular, humoral and innate immune responses has been leading the scientific discussion in the field of vaccine development.[46–48] Therefore, in addition to the determination of T cell responses, the murine sera from the immunization studies were analyzed for the presence of antigen-specific antibodies.

As expected for the positive control, polyfunctional CD4$^+$ IFN-γ^+ TNF-α^+ T cell responses were detected in mice vaccinated with the reference peptide plus ODN1826 mixture. TNF-α^+ and IL-17$^+$ CD4$^+$ T cell responses were also identified in mice immunized with either p57-UPam conjugate or mixture of p57 peptide plus UPam, indicating the development of a Th17 polarized cellular immune response. The significance of Th17 immunity for protection against *Mtb* is somewhat debated, with studies supporting its beneficial effect during early phases of mycobacterial

infection, and others indicating that it might lead to increased immunopathology and tissue destruction.[49–51]

Nevertheless, in addition to the $CD4^+$ T cell responses, the UPam conjugate induced very strong antibody responses, with multiple antigen-specific IgG subtypes found in sera of vaccinated mice. As opposed to mice vaccinated with the mixture of peptide plus UPam, where only IgG1 and IgG2b antibodies were found, mice vaccinated with the conjugate developed high titer IgG1, IgG2a, IgG2b, IgG2c and IgG3 antigen-specific antibodies. Importantly, high antibody titers against the cell lysate from heat-killed *Mtb* were detected in the case of IgG1 and IgG2b subtypes found in the sera of mice vaccinated with the conjugate. Traditionally, murine IgG1 are associated with a Th2 polarized immune response, while IgG2b antibodies are thought to be derived from T cell independent responses.[52–54] In 2016 Collins suggested a model of murine IgG function, called the quartet model, to integrate the beneficial effect of co-expression of different IgG subclasses. As formulated in Collins' paper, IgG3 and IgG2b antibody subclasses would play an important role in the early immune response, when cellular immune responses are slowly building up. In the specific, Collins underlined that IgG3 antibodies are associated with complement fixation, and IgG2b antibodies with early FcγR-mediated effector functions. On the other hand, IgG2a and IgG1 antibodies, which are defined as two murine T cell-mediated subclasses, would come into play in late immune responses. In fact, IgG2a has been shown to be involved both in complement fixation and late FcγR-mediated effector functions. Although the role of IgG1 in immune protection is currently debated, due to its inability to fix complement and its binding to the inhibitory FcγRIIb receptor, Collins suggested that it could well be involved in limiting inflammation and immunopathology. [55]

Perhaps the most important evidence supporting vaccine efficacy of the UPam conjugate was obtained in the murine *in vivo Mtb* challenge model, in which immunized mice were exposed to a high dose (10^5 CFU) of *Mtb* intranasally. The significant reduction in bacterial load in the spleen of conjugate-immunized mice was indicative of a systemic immune response, with significantly better results obtained for this treatment as compared to both the unconjugated peptide/UPam mixture, as well as the unconjugated peptide mixed with ODN1826. In 2019, Ashhurst *et al.* published a study showing that intranasal immunization using a Pam_2Cys-peptide conjugate was superior to subcutaneous immunization, by inducing stronger Th17 cellular responses and providing better protection against mycobacterial infection.[56] As opposed to the experiments reported in this chapter, which employ a TLR2/TLR1 ligand, their experiments were performed using a TLR2/TLR6 adjuvant, lower dose (10^2 CFU) nasal *Mtb* infection and a different oligopeptide. Nevertheless, their promising results, where protection against *Mtb* is evident also in the lung of vaccinated mice, further supports the potential of synthetic conjugates containing toll-like receptor ligands for the development of novel

vaccines against TB. Their research, published after the execution of the experiments reported in this chapter, combined with the reported observations, provides useful insights for possible next steps such as to assess the vaccine potential of the p57-UPam conjugate as intranasal vaccine and the development of second-generation synthetic conjugates including additional (synergistic) adjuvants and/or epitopes that can be presented by multiple HLA class II cell molecules.

Conclusion

In search for an effective conjugate vaccine against tuberculosis, a panel of three synthetic conjugates containing a TLR2 ligand covalently attached to one of three antigenic peptides was designed (p57 from the *Mtb* Rv1733c protein, p31 and p75 from the Rv2034 protein). In the present study, it is reported that these conjugates induced activation and maturation of human monocyte-derived dendritic cells *in vitro*, with production of IL-12p40 and IL-10 cytokines. Moreover, they were able to activate human monocyte-derived macrophages type 1 and type 2 yielding similar activation profiles to those of the adjuvant alone, an indication that the adjuvanticity of the TLR2 ligand was preserved even when the adjuvant was covalently linked to the peptide. Importantly, peptide antigen processing by monocytes and dendritic cells, and presentation to T lymphocytes were not impaired by conjugation, as determined by *in vitro* T cell antigen presentation experiments with a *Mtb* Rv2034-specific human $CD4^+$ T cell clone. To further assess the vaccine potential of the new conjugates, *in vivo* subcutaneous immunization experiments were performed in mice using one of the three constructs as a proof of concept. Comparison of cellular and humoral immunity elicited in response to this conjugate and in response to the mixture of peptide with adjuvant indicated the superior efficacy of the synthetic conjugate strategy when compared to the mixture. Vaccination with the conjugate resulted in a strong Th17 cellular response and multifunctional T lymphocytes in the spleen, in addition to the presence of several diverse subtypes of peptide-specific IgG antibodies in sera. Finally, immunization with this construct induced a significant reduction of the bacterial load in the spleen of intranasally *Mtb* challenged mice, not seen in response to the unconjugated components. These data suggest a promising role for TLR2 ligand-peptide synthetic conjugates as a novel TB vaccine approach.

Materials and methods

Synthetic methods

Materials and methods for the synthesis of peptides and conjugates

Description of materials, analytical tools and general synthetic methods are provided in the "Materials for the synthesis of peptides and conjugates" and "General methods for the synthesis of peptides" sections of Chapter 3.

p57 peptide: Ile-Pro-Phe-Ala-Ala-Ala-Ala-Gly-Thr-Ala-Val-Gln-Asp-Ser-Arg-Ser-His-Val-Tyr-Ala-His-Gln-Ala-Gln-Thr-Arg- His-Pro-NH_2

The p57 peptide was synthesized according to the general procedure for peptide synthesis described above. Pseudoproline dipeptides Fmoc-Asp(OtBu)-Ser(ψMe,Mepro)-OH and Fmoc-Gly-Thr(ψMe,Mepro)-OH were employed to enhance synthetic efficiency. Purification by RP-HPLC (linear gradient 20→30% B in 10 min) followed by lyophilization yielded the p57 peptide as a white powder (90.4 mg, 30.26 μmol, 12.1% yield based on theoretical resin loading of 0.23 mmol/g). LC-MS analysis (C18 column, linear gradient 10→90% B, 11 min): Rt = 3.571 min, ESI-MS $[M+H]^{2+}$ = 1494.3 found, 1493.8 calculated. MALDI-TOF $[M+H]^{+}$: 2986.4517 found, 2986.5143 calculated.

p31 peptide: Leu-Ala-Val-Gly-Glu-Leu-Ala-Arg-Asp-Leu-Pro-Val-Ser-Arg-Pro-Ala-Val-Ser-Gln-His-Leu-Lys-Val-Leu-Lys-Thr-Ala-Arg-Leu-Val

The p31 peptide was synthesized according to the general procedure for peptide synthesis described above. TentaGel™ S PHB-Val-Fmoc resin was used in place of TentaGel® S RAM. Purification by RP-HPLC (linear gradient 20→35% B in 10 min) followed by lyophilization yielded the p31 peptide as a white powder (3.9 mg, 1.20 μmol, 12.0% yield based on theoretical resin loading of 0.19 mmol/g). LC-MS analysis (C18 column, linear gradient 10 → 50% B, 11 min): Rt = 5.895 min, ESI-MS $[M+H]^{2+}$ = 1619.5 found, 1618.5 calculated. MALDI-TOF $[M+H]^{+}$: 3237.425 found, 3236.932 calculated.

p75 peptide: Thr-Gly-Leu-Ala-Ala-Leu-Arg-Thr-Asp-Leu-Asp-Arg-Phe-Trp-Thr-Arg-Ala-Leu-Thr-Gly-Tyr-Ala-Gln-Leu-Ile-Asp-Ser-Glu-Gly-Asp-NH_2

The p75 peptide was synthesized according to the general procedure for peptide synthesis described above. Pseudoproline dipeptides Fmoc-Asp(OtBu)-Ser(ψMe,Mepro)-OH and Fmoc-Leu-Thr(ψMe,Mepro)-OH were employed to enhance synthetic efficiency. Purification by RP-HPLC (linear gradient 30→45% B in 10 min) followed by lyophilization yielded the p75 peptide as a white powder (11.7 mg, 3.53 μmol, 14.1% yield based on theoretical resin loading of 0.23 mmol/g). LC-MS analysis (C18 column, linear gradient 10→90% B, 11 min): Rt = 5.508 min, ESI-MS $[M+H]^{2+}$ = 1663.4 found, 1662.9 calculated. MALDI-TOF $[M+H]^{+}$: 3325.092 found, 3324.693 calculated.

UPam (Amplivant) synthesis

Compound UPam was synthesized according to published protocol and analytical data were in agreement with those published in the literature.[17]

General methods for UPam-conjugates synthesis

Peptide sequence was synthesized according to the general procedure for peptide synthesis described in Chapter 3. After completion of all the synthetic cycles, the peptide was not cleaved from the resin. Instead, the resin was treated with a 0.1 M stock solution of Fmoc-Cys((RS)-2,3-di(palimitoyloxy)-propyl)-OH (2eq) and in the presence of oxyma pure (1 M, 1 eq) and DIC (0.5 M, 1 eq), with the reaction being performed overnight at RT. After NMP and DCM washes, the resin was swelled in a mixture of DCM/NMP 2:1 and treated with 20% piperidine in NMP (3 times, 5 minutes) to remove Fmoc protecting groups. After NMP wash the resin was suspended in DCM/NMP 1:1 (1 ml per 10 µmol resin) and treated with tetradecyl isocyanate (25 µl per 25 µmol resin). The mixture was reacted for 6 hours at RT, washed with NMP and DCM and air dried. The resin was then treated for 1 hour and 30 minutes with a TFA/TIS/H_2O (38:1:1, v/v/v) cleavage cocktail (5 ml/100 µmol scale reaction). The reaction mixture containing the cleaved peptide was filtered into cold Et_2O/pentane (1/1, v/v) (50 mL/1 ml cleavage cocktail) and the resin was washed with 1 mL TFA (2 times) into the cold Et_2O/pentane solution. The solution was stored in a -20°C freezer for 2 hours, then centrifuged (10 minutes, 4400 rpm, 3 x g); finally, the supernatant was discarded and the precipitate was purified via RP-HPLC.

p57-UPam conjugate: UPam-Ser-Lys-Lys-Lys-Lys-Ile-Pro-Phe-Ala-Ala-Ala-Ala-Gly-Thr-Ala-Val-Gln-Asp-Ser-Arg-Ser-His-Val-Tyr-Ala-His-Gln-Ala-Gln-Thr-Arg-His-Pro-NH_2

Purification by RP-HPLC (C4 column, linear gradient 50→90% B in 10 min) followed by lyophilization yielded p57-UPam conjugate as a white powder (15.1 mg, 3.35 µmol, 3.3% yield based on theoretical resin loading of 0.23 mmol/g). LC-MS analysis (C4 column, linear gradient 25→75% B, 21 min): Rt = 8.737 min, ESI-MS $[M+H]^{3+}$ = 1494.2 found, 1493.9 calculated. MALDI-TOF $[M+H]^{+}$: 4478.5690 found, 4478.6563 calculated.

p31-UPam conjugate: UPam-Ser-Lys-Lys-Lys-Lys-Leu-Ala-Val-Gly-Glu-Leu-Ala-Arg-Asp-Leu-Pro-Val-Ser-Arg-Pro-Ala-Val-Ser-Gln-His-Leu-Lys-Val-Leu-Lys-Thr-Ala-Arg-Leu-Val

TentaGel™ S PHB-Val-Fmoc resin was used in place of TentaGel® S RAM. Purification by RP-HPLC (C4 column, linear gradient 50→90% B in 10 min) followed by lyophilization yielded p31-UPam conjugate as a white powder (34.5 mg,7.27 µmol, 7.3% yield based on theoretical resin loading of 0.19 mmol/g). LC-MS analysis (C4 column, linear gradient 50→90% B, 15 min): Rt = 8.910 min, ESI-MS $[M+H]^{3+}$ = 1577.9 found, 1577.0 calculated. MALDI-TOF $[M+H]^{+}$: 4729.1481 found, 4729.0744calculated.

p75-UPam conjugate: UPam-Ser-Lys-Lys-Lys-Lys-Thr-Gly-Leu-Ala-Ala-Leu-Arg-Thr-Asp-Leu-Asp-Arg-Phe-Trp-Thr-Arg-Ala-Leu-Thr-Gly-Tyr-Ala-Gln-Leu-Ile-Asp-Ser-Glu-Gly-Asp-NH_2

Purification by RP-HPLC (C4 column, linear gradient 50→90% B in 10 min) followed by lyophilization yielded SLP3-UPam as a white powder (7.0 mg, 1.4 µmol, 2.8% yield based on theoretical resin loading of 0.23 mmol/g). LC-MS analysis (C4 column, linear gradient 10→90% B, 21 min): Rt = 12.688 min, ESI-MS $[M+H]^{3+}$ = 1607.0 found, 1606.3 calculated. MALDI-TOF $[M+H]^{+}$: 4816.6670 found, 4816.8392 calculated.

Immunological methods

Culturing of HEK-293 cell line

The HEK-293-h-TLR2 and HEK-293-null cell lines were purchased from InvivoGen (San Diego, United States) and cultured according to manufacturer's instructions. DMEM (Gibco, PAA, Linz, Austria) culture medium contained: 4.5 g/l glucose, 10% (v/v) fetal calf serum (FCS) (HyClone, GE Healthcare Life Sciences, Eindhoven, the Netherlands), 50 U/ml penicillin, 50 mg/ml streptomycin, 100 mg/ml Normocin and 2 mM L-glutamine (Life Technologies-Invitrogen, Bleiswijk, the Netherlands).

Stimulation of HEK-293 cells

Approximately 20.000 cells/well were transferred to 96 well plates (flat bottom, Corning Costar TC-Treated Microplates, Corning, NY, USA). All compounds used for stimulation were pre-dissolved in DMSO (Sigma, St.Louis, MO, USA) at a concentration of 5 nmol/μL and subsequently diluted in culture medium. Reference peptides were used as negative controls. After overnight stimulation with UPam and UPam conjugates, supernatants were harvested for IL-8 cytokine detection.

Generation and stimulation of immature human moDCs and macrophages

Human moDCs and GM-CSF/M-CSF macrophages were generated as described in "Generation and stimulation of immature human moDCs and macrophages" section in Chapter 3. Cells were stimulated using synthetic compounds (at concentrations ranging from 20-1-0.05 μM). The synthetic compounds were dissolved in DMSO at a concentration of 5 nmol/μL, further diluted and premixed in RPMI 1640 medium containing 10% FCS, 2 mM GlutaMAX™, 1% Pen-Strep. LPS (100 ng/ml) was used as positive control for stimulated cells. Supernatants were harvested 20 hours after the addition of stimuli for subsequent analysis of cytokines and cells were stained as described in Flow cytometric analysis of human moDCs and macrophages section in Chapter 3.

Human IL-8, IL-12(p40) and IL-10 ELISA

Human IL-8 Elisa kit was purchased from R&D Systems (Abingdon, UK). Human IL-12/IL-23 (p40) and human IL-10 ELISA kits were purchased from Biolegend (ELISA MAX™ Standard Set; London, UK). All supernatants were tested in duplicates according to manufacturer's instructions. Sample absorbance was measured using a Spectramax i3x (Molecular Devices, CA, USA) spectrometer.

T cell proliferation

T cell proliferation was assessed by coculturing 2500 HLA-DR3 matched monocyte derived dendritic cells or $5x10^4$ irradiated (2000 rad), HLA-DR3 matched PBMC's with 10^4 T cells from an established T cell clone specific for peptide 75-105 of Rv2034 from *M.tuberculosis*, in a 96 well round bottom plate in the absence or presence of serial dilutions of UPam conjugated peptides. Cells were cultured in IMDM supplemented with Glutamax, 100 U/ml penicillin, 100 μg/ml streptomycin (Gibco, Thermo Fisher Scientific, Bleiswijk, the Netherlands) and 10% pooled human serum (Sigma, Merck, Darmstadt, Germany) for a total of 96 hours in a humidified incubator at 37°C and 5% CO_2. After 72 hours [^{3}H]-Thymidine (Perkin Elmer,

Groningen, the Netherlands) was added at 0.5µCi/well. Following an additional 18 hours of incubation cells were harvested with a TomTec cell harvester and measured on a MicroBetaPlate Scintillation counter 1450 (Wallac, Turku, Finland). Data is represented as mean counts per minute from triplicate wells.

Flowcytometric antigen specificity analysis

HLA-DR3$^+$ monocyte derived dendritic cells were cocultured with the different peptides and peptide conjugates and 1x10^5 T cells from the Rv2034 specific T cell clone (recognizing peptide 75-105) in a 5 ml Falcon tube in a total volume of 400 µl IMDM supplemented with Glutamax, 100 U/ml penicillin, 100 µg/ml streptomycin (Gibco, Thermo Fisher Scientific, Bleiswijk, the Netherlands) and 10% pooled human serum (Sigma, Merck, Darmstadt, Germany). After 6 hours Brefeldin-A was added (3 µg/ml) (Sigma, Merck, Darmstadt, Germany) and cells were incubated for an additional 16 hours. Subsequently cells were harvested and stained for flowcytometric analysis with the violet live/dead stain (ViViD, Invitrogen, Thermo Fisher Scientific, Bleiswijk, the Netherlands), surface markers CD3-HorizonV500 (clone UCHT; BD Biosciences, San Diego, CA, USA), CD4-AlexaFluor 700 (clone RPAT4; BD Biosciences), CD8-FITC (clone HIT8a; Biolegend) and after fixation and permeabilization with fix/perm reagents (Nordic MUbio, Susteren, the Netherlands) for IFN-ϒ-PerCP-Cy5.5 (clone B27; BD Biosciences) and CD154-PE (clone TRAP1; BD Biosciences). Cells were acquired on a LSRFortessa with FACSDiva vxx and analyzed with Flowjo v9.7.6 (Treestar Inc, Ashland, OR, USA)

Mice

HLA-DRB1*0301/DRA transgenic, murine class II-deficient (HLA-DR3/Ab^0) mice were bred and PBMCs of each mouse were typed for expression and segregation of the transgene as described in Mice section in Chapter 3.

Immunizations

Mice (3 to 6 animals per group; 6 weeks old) were injected subcutaneously in the right flank with conjugate, or mixtures of p57-peptide and UPam adjuvant, in 200 µl phosphate-buffered saline (PBS) at 2 weeks interval. Two weeks after the last immunization, splenocytes were harvested.

In vitro culture, stimulation and intracellular cytokine staining of splenocytes

Splenocytes were isolated and incubated with medium, peptide, or relevant recombinant *Mtb* protein as described in the "In vitro cultures of splenocytes" section in Chapter 3. Intracellular cytokine staining was performed as described in the Intracellular cytokine staining section in Chapter 3.

Antibody detection

Antibodies against the Rv1733c p57 peptide, Rv1733c protein and *Mtb* sonicate in serum from immunized mice were determined by ELISA as described in "Antibody detection" section in Chapter 3.

BCG immunization and intranasal infection of mice with live Mtb

See section "BCG immunization and intranasal infection of mice with live Mtb" in Chapter 3.

Supporting figures

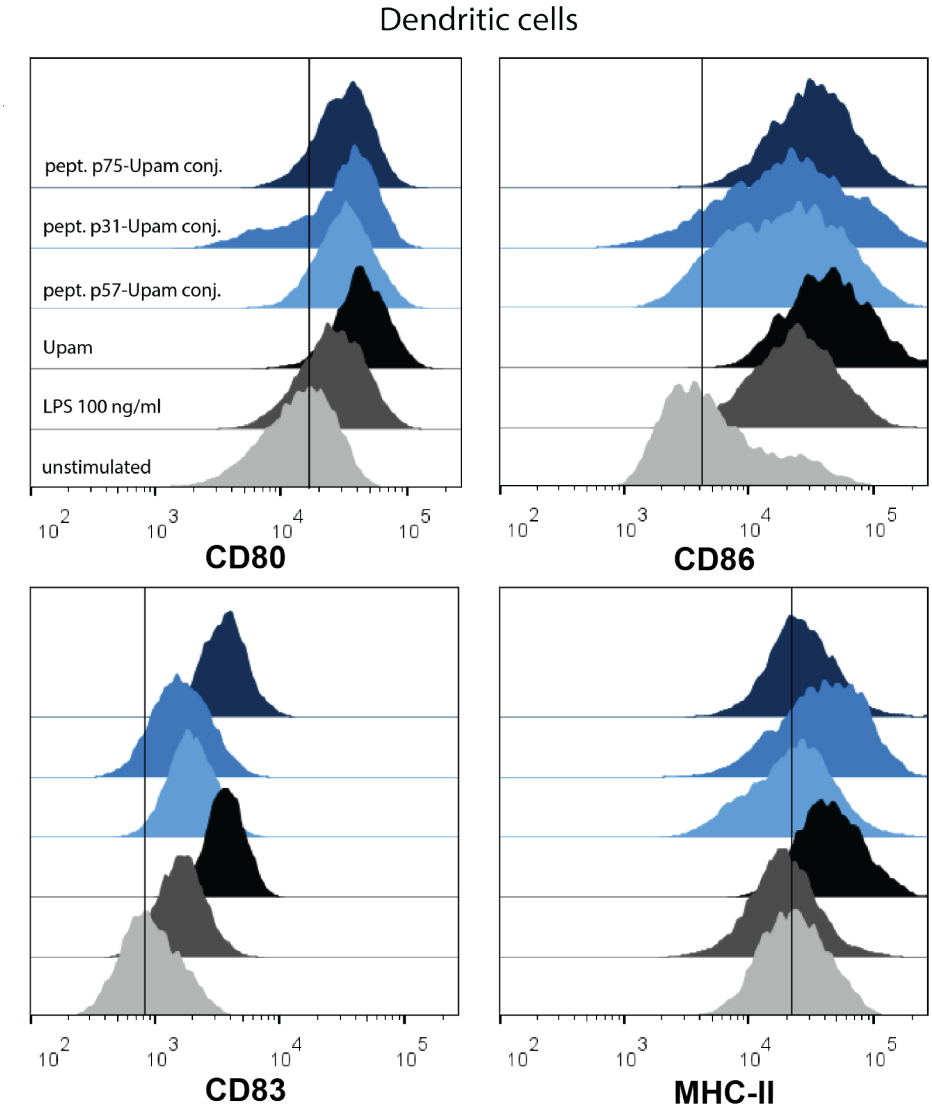

S1 Figure - Expression of activation or T cell costimulatory markers by DCs as measured by flow cytometry. UPam (20 μM) and synthetic conjugates (20 μM) are used to stimulate human monocyte-derived dendritic cells. LPS (100ng/ml) was used as positive control. Representative data from one of three human donors are shown.

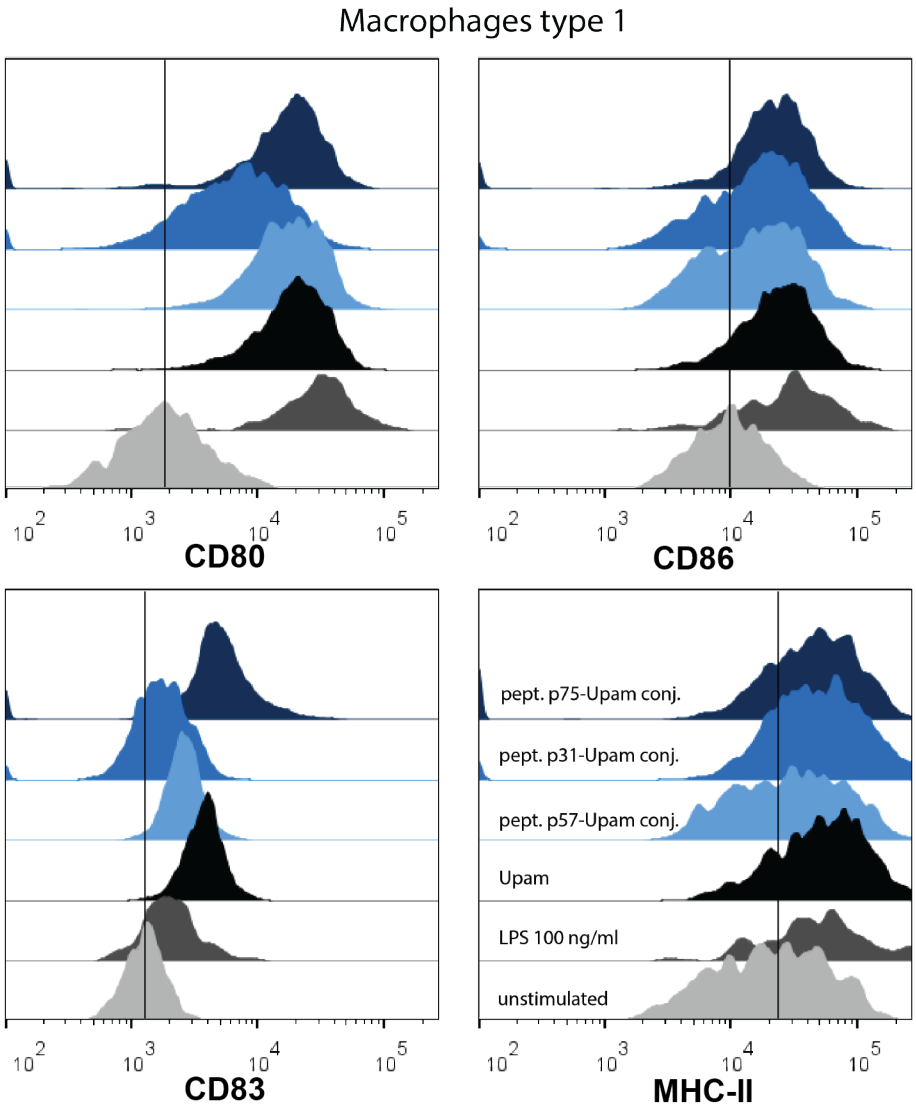

S2 Figure - Expression of activation or T cell costimulatory markers by GM-CSF/M1 macrophages as measured by flow cytometry. UPam (20 µM) and synthetic conjugates (20 µM) are used to stimulate human monocyte-derived macrophages type 1. LPS (100ng/ml) was used as positive control. Representative data from one of three human donors are shown.

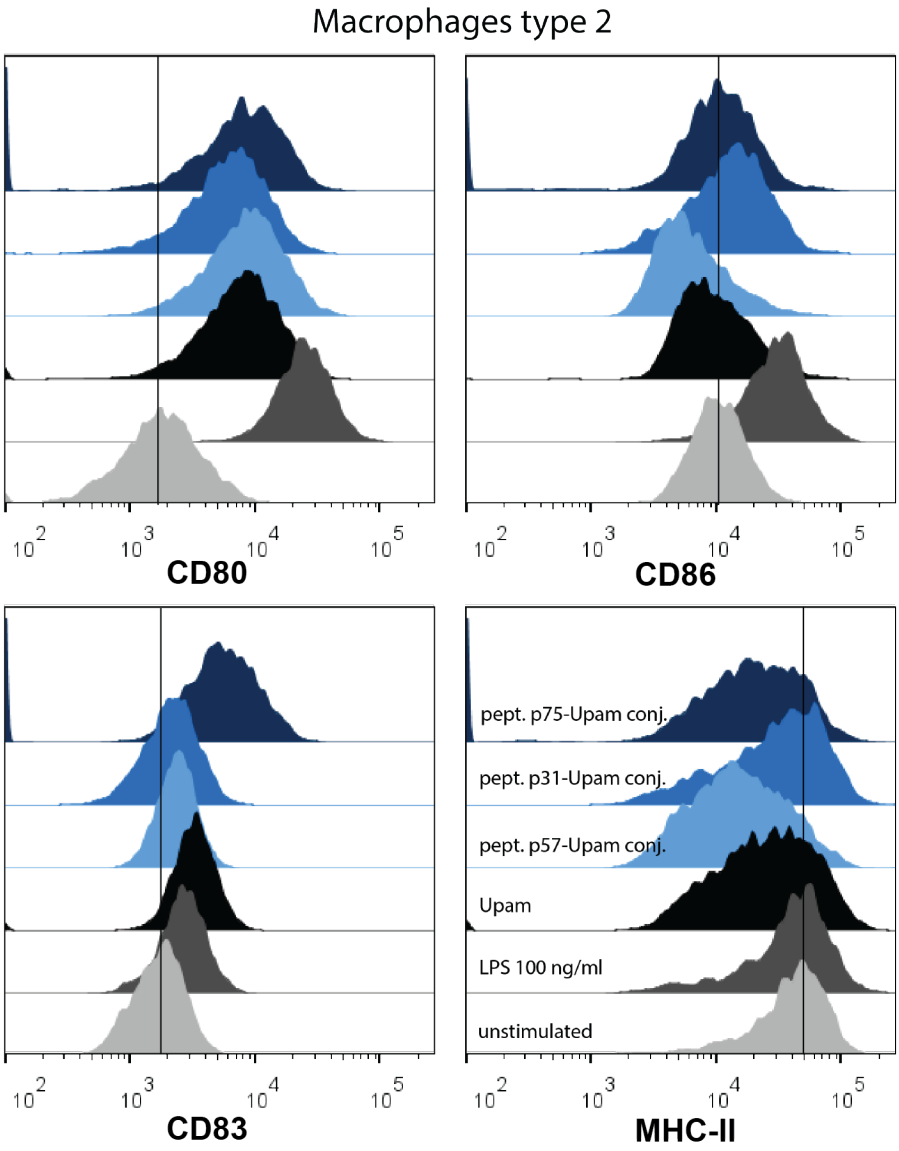

S3 Figure - Expression of activation or T cell costimulatory markers by M-CSF/M2 macrophages as measured by flow cytometry. UPam (20 μM) and synthetic conjugates (20 μM) are used to stimulate human monocyte-derived macrophages type 2. LPS (100ng/ml) was used as positive control. Representative data from one of three human donors are shown.

References

1. Geneva: World Health Organization. Global tuberculosis report 2020. 2020.

2. Andersen P, Kaufmann SHE. Novel Vaccination Strategies against Tuberculosis. Cold Spring Harb Perspect Med. 2014 Jun 1;4(6):a018523–a018523.

3. Rappuoli R, De Gregorio E, Del Giudice G, Phogat S, Pecetta S, Pizza M, et al. Vaccinology in the post–COVID-19 era. Proc Natl Acad Sci. 2021 Jan 19;118(3):e2020368118.

4. Verbeke R, Lentacker I, De Smedt SC, Dewitte H. The dawn of mRNA vaccines: The COVID-19 case. J Controlled Release. 2021 May;333:511–20.

5. Rueckert C, Guzmán CA. Vaccines: From Empirical Development to Rational Design. PLoS Pathog. 2012 Nov 8;8(11):e1003001.

6. Jones LH. Recent advances in the molecular design of synthetic vaccines. Nat Chem. 2015 Dec;7(12):952–60.

7. Jiang Z-H, Koganty R. Synthetic Vaccines: The Role of Adjuvants in Immune Targeting. Curr Med Chem. 2003 Aug 1;10(15):1423–39.

8. Skwarczynski M, Toth I. Peptide-based synthetic vaccines. Chem Sci. 2016;7(2):842–54.

9. Hancock G, Hellner K, Dorrell L. Therapeutic HPV vaccines. Best Pract Res Clin Obstet Gynaecol. 2018 Feb;47:59–72.

10. Ouerfelli O, Warren JD, Wilson RM, Danishefsky SJ. Synthetic carbohydrate-based antitumor vaccines: challenges and opportunities. Expert Rev Vaccines. 2005 Oct;4(5):677–85.

11. Quakkelaar ED, Melief CJM. Experience with Synthetic Vaccines for Cancer and Persistent Virus Infections in Nonhuman Primates and Patients. In: Advances in Immunology. Elsevier; 2012. p. 77–106.

12. Yamamoto M, Sato S, Hemmi H, Sanjo H, Uematsu S, Kaisho T, et al. Essential role for TIRAP in activation of the signalling cascade shared by TLR2 and TLR4. Nature. 2002 Nov;420(6913):324–9.

13. van Bergenhenegouwen J, Plantinga TS, Joosten LAB, Netea MG, Folkerts G, Kraneveld AD, et al. TLR2 & Co: a critical analysis of the complex interactions between TLR2 and coreceptors. J Leukoc Biol. 2013 Nov;94(5):885–902.

14. Zom GG, Khan S, Britten CM, Sommandas V, Camps MGM, Loof NM, et al. Efficient Induction of Antitumor Immunity by Synthetic Toll-like Receptor Ligand–Peptide Conjugates. Cancer Immunol Res. 2014 Aug;2(8):756–64.

15. Zom GG, Welters MJ, Loof NM, Goedemans R, Lougheed S, Valentijn RR, et al. TLR2 ligand-synthetic long peptide conjugates effectively stimulate tumor-draining lymph node T cells of cervical cancer patients. Oncotarget. 2016 Oct;7(41):67087.

16. Tyne AS, Chan JGY, Shanahan ER, Atmosukarto I, Chan H-K, Britton WJ, et al. TLR2-targeted secreted proteins from *Mycobacterium tuberculosis* are protective as powdered pulmonary vaccines. Vaccine. 2013 Sep;31(40):4322–9.

17. Willems MM, Zom GG, Khan S, Meeuwenoord N, Melief CJ, van der Stelt M, et al. N-tetradecylcarbamyl lipopeptides as novel agonists for toll-like receptor 2. J Med Chem. 2014 Jul;57(15):6873–8.

18. Palomo JM. Solid-phase peptide synthesis: an overview focused on the preparation of biologically relevant peptides. RSC Adv. 2014;4(62):32658–72.

19. Ottenhoff THM, Elferink DG, Hermans J, de Vries RRP. HLA class II restriction repertoire of antigen-specific T cells. I. The main restriction determinants for antigen presentation are associated with HLA-D/DR and not with DP and DQ. Hum Immunol. 1985 Jun;13(2):105–16.

20. Commandeur S, van Meijgaarden KE, Prins C, Pichugin AV, Dijkman K, van den Eeden SJF, et al. An Unbiased Genome-Wide *Mycobacterium tuberculosis* Gene Expression Approach To Discover Antigens Targeted by Human T Cells Expressed during Pulmonary Infection. J Immunol. 2013 Feb 15;190(4):1659–71.

21. Commandeur S, van den Eeden SJF, Dijkman K, Clark SO, van Meijgaarden KE, Wilson L, et al. The in vivo expressed *Mycobacterium tuberculosis* (IVE-TB) antigen Rv2034 induces CD4+ T-cells that protect against pulmonary infection in HLA-DR transgenic mice and guinea pigs. Vaccine. 2014 Jun;32(29):3580–8.

22. Coppola M, van den Eeden SJF, Wilson L, Franken KLMC, Ottenhoff THM, Geluk A. Synthetic Long Peptide Derived from *Mycobacterium tuberculosis* Latency Antigen Rv1733c Protects against Tuberculosis. Pascual DW, editor. Clin Vaccine Immunol. 2015 Sep;22(9):1060–9.

23. Coppola M, van Meijgaarden KE, Franken KLMC, Commandeur S, Dolganov G, Kramnik I, et al. New Genome-Wide Algorithm Identifies Novel In-Vivo Expressed *Mycobacterium Tuberculosis* Antigens Inducing Human T-Cell Responses with Classical and Unconventional Cytokine Profiles. Sci Rep. 2016 Dec;6(1):37793.

24. Black GF, Thiel BA, Ota MO, Parida SK, Adegbola R, Boom WH, et al. Immunogenicity of Novel DosR Regulon-Encoded Candidate Antigens of *Mycobacterium tuberculosis* in Three High-Burden Populations in Africa. Clin Vaccine Immunol. 2009 Aug;16(8):1203–12.

25. Commandeur S, Coppola M, Dijkman K, Friggen AH, van Meijgaarden KE, van den Eeden SJF, et al. Clonal Analysis of the T-Cell Response to In Vivo Expressed *Mycobacterium tuberculosis* Protein Rv2034, Using a CD154 Expression Based T-Cell Cloning Method. PLoS ONE. 2014 Jun 6;9(6):e99203.

26. Verreck FA, de Boer T, Langenberg DM, Hoeve MA, Kramer M, Vaisberg E, et al. Human IL-23-producing type 1 macrophages promote but IL-10-producing type 2 macrophages subvert immunity to (myco) bacteria. Proc Natl Acad Sci. 2004 Mar;101(13):4560–5.

27. Verreck FA, de Boer T, Langenberg DM, van der Zanden L, Ottenhoff TH. Phenotypic and functional profiling of human proinflammatory type-1 and anti-inflammatory type-2 macrophages in response to microbial antigens and IFN-γ-and CD40L-mediated costimulation. J Leukoc Biol. 2006 Feb;79(2):285–93.

28. Geluk A, Taneja V, van Meijgaarden KE, Zanelli E, Abou-Zeid C, Thole JER, et al. Identification of HLA class II-restricted determinants of *Mycobacterium tuberculosis*-derived proteins by using HLA-transgenic, class II-deficient mice. Proc Natl Acad Sci. 1998 Sep 1;95(18):10797–802.

29. Budd RC, Cerottini JC, Horvath C, Bron C, Pedrazzini T, Howe RC, et al. Distinction of virgin and memory T lymphocytes. Stable acquisition of the Pgp-1 glycoprotein concomitant with antigenic stimulation. J Immunol. 1987 May 15;138(10):3120.

30. Andersen P, Doherty TM. The success and failure of BCG — implications for a novel tuberculosis vaccine. Nat Rev Microbiol. 2005 Aug;3(8):656–62.

31. Hesseling AC, Marais BJ, Gie RP, Schaaf HS, Fine PEM, Godfrey-Faussett P, et al. The risk of disseminated Bacille Calmette-Guerin (BCG) disease in HIV-infected children. Vaccine. 2007 Jan;25(1):14–8.

32. Martin C, Aguilo N, Marinova D, Gonzalo-Asensio J. Update on TB Vaccine Pipeline. Appl Sci. 2020 Apr 10;10(7):2632.

33. Li J, Zhao A, Tang J, Wang G, Shi Y, Zhan L, et al. Tuberculosis vaccine development: from classic to clinical candidates. Eur J Clin Microbiol Infect Dis. 2020 Aug;39(8):1405–25.

34. Vetter V, Denizer G, Friedland LR, Krishnan J, Shapiro M. Understanding modern-day vaccines: what you need to know. Ann Med. 2018 Feb 17;50(2):110–20.

35. Stewart E, Triccas JA, Petrovsky N. Adjuvant Strategies for More Effective Tuberculosis Vaccine Immunity. Microorganisms. 2019 Aug 12;7(8):255.

36. Del Giudice G, Rappuoli R, Didierlaurent AM. Correlates of adjuvanticity: A review on adjuvants in licensed vaccines. Semin Immunol. 2018 Oct;39:14–21.

37. Mishra A, Akhtar S, Jagannath C, Khan A. Pattern recognition receptors and coordinated cellular pathways involved in tuberculosis immunopathogenesis: emerging concepts and perspectives. Mol Immunol. 2017 Jul;87:240–8.

38. Irvine DJ, Swartz MA, Szeto GL. Engineering synthetic vaccines using cues from natural immunity. Nat Mater. 2013 Nov;12(11):978–90.

39. Zhang Y, Luo F, Cai Y, Liu N, Wang L, Xu D, et al. TLR1/TLR2 Agonist Induces Tumor Regression by Reciprocal Modulation of Effector and Regulatory T Cells. J Immunol. 2011 Feb 15;186(4):1963–9.

40. Wang Z-B, Xu J. Better Adjuvants for Better Vaccines: Progress in Adjuvant Delivery Systems, Modifications, and Adjuvant–Antigen Codelivery. Vaccines. 2020 Mar 13;8(1):128.

41. Ma X, Yan W, Zheng H, Du Q, Zhang L, Ban Y, et al. Regulation of IL-10 and IL-12 production and function in macrophages and dendritic cells. F1000Research. 2015 Dec 17;4:1465.

42. Groux H, Bigler M, de Vries JE, Roncarolo M-G. Inhibitory and Stimulatory Effects of IL-10 on Human $CD8^+$ T Cells. J Immunol. 1998 Apr 1;160(7):3188.

43. Santin AD, Hermonat PL, Ravaggi A, Bellone S, Pecorelli S, Roman JJ, et al. Interleukin-10 Increases Th1 Cytokine Production and Cytotoxic Potential in Human Papillomavirus-Specific $CD8^+$ Cytotoxic T Lymphocytes. J Virol. 2000 May 15;74(10):4729–37.

44. Ottenhoff THM. New pathways of protective and pathological host defense to mycobacteria. Trends Microbiol. 2012 Sep;20(9):419–28.

45. Ottenhoff THM, Kaufmann SHE. Vaccines against Tuberculosis: Where Are We and Where Do We Need to Go? PLoS Pathog. 2012 May 10;8(5):e1002607.

46. Nunes-Alves C, Booty MG, Carpenter SM, Jayaraman P, Rothchild AC, Behar SM. In search of a new paradigm for protective immunity to TB. Nat Rev Microbiol. 2014 Apr;12(4):289–99.

47. Divangahi M. Are tolerance and training required to end TB? Nat Rev Immunol. 2018 Nov;18(11):661–3.

48. Brazier B, McShane H. Towards new TB vaccines. Semin Immunopathol. 2020 Jun;42(3):315–31.

49. Khader SA, Bell GK, Pearl JE, Fountain JJ, Rangel-Moreno J, Cilley GE, et al. IL-23 and IL-17 in the establishment of protective pulmonary CD4+ T cell responses after vaccination and during Mycobacterium tuberculosis challenge. Nat Immunol. 2007 Apr;8(4):369–77.

50. Cruz A, Fraga AG, Fountain JJ, Rangel-Moreno J, Torrado E, Saraiva M, et al. Pathological role of interleukin 17 in mice subjected to repeated BCG vaccination after infection with *Mycobacterium tuberculosis*. J Exp Med. 2010 Aug 2;207(8):1609–16.

51. Torrado E, Robinson RT, Cooper AM. Cellular response to mycobacteria: balancing protection and pathology. Trends Immunol. 2011 Feb;32(2):66–72.

52. Snapper CM, Mond JJ. Towards a comprehensive view of immunoglobulin class switching. Immunol Today. 1993 Jan;14(1):15–7.

53. Mosmann T. TH1 and TH2 cells: different patterns of lymphokine secretion lead to different functional properties. Annu Rev Immunol. 1989 Apr;

54. Deenick EK, Hasbold J, Hodgkin PD. Switching to IgG3, IgG2b, and IgA is division linked and independent, revealing a stochastic framework for describing differentiation. J Immunol Baltim Md 1950. 1999 Nov 1;163(9):4707–14.

55. Collins AM. IgG subclass co-expression brings harmony to the quartet model of murine IgG function. Immunol Cell Biol. 2016 Nov;94(10):949–54.

56. Ashhurst AS, McDonald DM, Hanna CC, Stanojevic VA, Britton WJ, Payne RJ. Mucosal Vaccination with a Self-Adjuvanted Lipopeptide Is Immunogenic and Protective against *Mycobacterium tuberculosis*. J Med Chem. 2019 Sep 12;62(17):8080–9.